Dalton Transactions

Dual-Action Organoplatinum Polymeric Nanoparticles Overcoming Drug Resistance in Ovarian Cancer

Journal:	*Dalton Transactions*
Manuscript ID	DT-ART-04-2019-001683.R1
Article Type:	Paper
Date Submitted by the Author:	01-Jul-2019
Complete List of Authors:	Zheng, Yaorong; Kent State University, Jayawardhana, Amarasooriya ; Kent State University Qiu, Zihan; Kent State University Kempf, Susan; Kent State University Wang, Han; Kent State University Bowers, David; Kent State University Miterko, Mitchell; Kent State University

Journal Name

ARTICLE

Dual-Action Organoplatinum Polymeric Nanoparticles Overcoming Drug Resistance in Ovarian Cancer

Received 00th January 20xx,
Accepted 00th January 20xx

DOI: 10.1039/x0xx00000x

www.rsc.org/

Amarasooriya M. D. S. Jayawardhanaa,[a] Zhihan Qiu,[a] Susan Kempf,[a] Han Wang,[a] Mitchell Miterko,[a] David J. Bowers,[a] and Yao-Rong Zheng *[a]

Drug resistance to the conventional platinum chemotherapy remains a major challenge for treating ovarian cancer. Herein, we present a novel approach to overcome drug resistance by utilizing "dual-action" organometallic polymeric nanoparticles (OPNPs). The OPNPs were formed by the assembly of the organoplatinum payloads and anionic block copolymer, methoxy polyethylene glycol-block-polyglutamic acid ($MPEG_{5k}$-PGA_{50}). The OPNPs enhance the solubility and biocompatibility of the hydrophobic organoplatinum payloads. The OPNPs enter cancer cells via endocytosis, and the payloads loaded in the core of the nanoparticles are slowly released under the acidic condition of endosomes. Unlike conventional platinum therapeutics, the organoplatinum compound exhibits a "dual-action" attack by triggering nuclear DNA damage and mitochondrial damage. As a result, drug-resistant ovarian cancer cells become vulnerable to the organoplatinum payloads.

Introduction

Drug resistance to the conventional platinum chemotherapy remains a major challenge for treating ovarian cancer.[1] The FDA-approved platinum therapeutics, cisplatin and carboplatin, are widely used as the first-line therapy for treating ovarian cancer.[2] Their anticancer activity arises from the nuclear DNA damage caused by the formation of intra- and interstrand DNA adducts between Pt and the purine nucleobases.[3] Despite good responses to initial treatments, approximately 70–80% of patients eventually develop drug resistance. The origin of drug resistance in ovarian cancer patients is still under exploration, but several mechanisms are commonly accepted in the field, and include decrease in drug uptake, enhanced DNA damage repair ability, and upregulation of anti-apoptotic proteins, drug efflux transporters and detoxifying enzymes/molecules.[4] Due to the lack of alternative treatments for drug-resistant ovarian tumors, patients who develop drug resistance are commonly diagnosed as incurable.

Organometallic complexes have recently received significant attention for their use as a new type of metallodrug in cancer therapy.[5-25] Compared to the conventional platinum drugs, organometallic compounds provide greater structural variety, and allow for the design of novel classes of anticancer agents. These complexes can be fine-tuned in various aspects attributing to their biological activities, including coordination geometry, stereochemistry, and ligand exchange kinetics.[9, 23] In the past, organometallic compounds of ruthenium and gold have been extensively explored for their potentials in cancer therapy.[11, 16, 20, 23-25] More recently, emerging studies have demonstrated the ample opportunities of engaging organoplatinum complexes in biomedical applications.[5, 22] In particular, the new studies conducted by Che, Das, Ruiz, and Stang, respectively, show that organoplatinum compounds are of significance as new therapeutics for breast cancer, anti-angiogenesis agents, and photodynamic therapy.[17, 26-36] However, reports about using organoplatinum complexes for treating drug-resistant ovarian cancer is still rare.[29]

In this study, we developed a novel approach to engage organoplatinum complexes as potential reagents to overcome the challenge of drug resistance in ovarian cancer. The innovation of this work is two-fold: First, we engineered novel organoplatinum polymeric nanoparticles (OPNPs, Fig 1) via the assembly of the organoplatinum complex (**1**) and anionic block copolymer, methoxy polyethylene glycol-block-polyglutamic acid ($MPEG_{5k}$-PGA_{50}, **2** in Fig 1). In the past, organoplatinum building blocks are frequently used in coordination-driven self-assembly.[35, 37-44] Instead of using small-molecule pyridyl/carboxylic linkers, we creatively used polymers with carboxylic groups as donors to coordinate to the platinum centres, which allows for self-assembly of large nanoparticles.[45] Taking advantage of the PEG moieties of the polymer, OPNPs are able to enhance solubility and biocompatibility of the hydrophobic organoplatinum payloads in aqueous solution. Second, we found that the platinum payloads released from the OPNPs carry out a "dual-action" attack by triggering nuclear DNA damage and mitochondrial damage. As a result, cisplatin-resistant ovarian cancer cells become vulnerable to these nanoparticles.

[a] Department of Chemistry and Biochemistry, Kent State University, 224 Williams Hall, Kent, Ohio 44242.
Email: yzheng7@kent.edu
Electronic Supplementary Information (ESI) available. See DOI: 10.1039/x0xx00000x

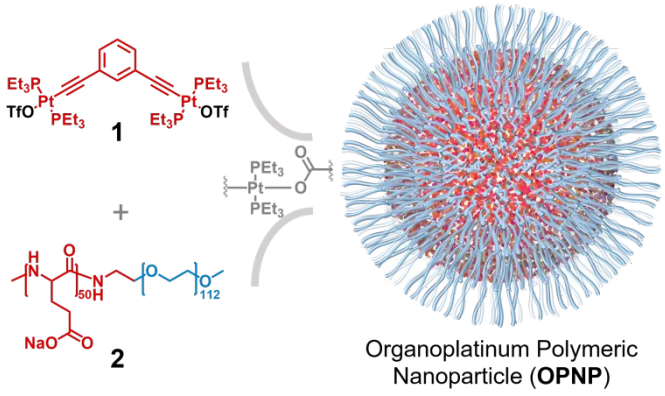

Figure 1. Nanoformulation of the organoplatinum polymeric nanoparticles (OPNPs) using organoplatinum build block (**1**) with block copolymer (**2**).

Results and discussion

Formulation of organoplatinum polymeric nanoparticles (OPNPs). The organoplatinum(II) building block (**1**, 1.7 µmol) and $MPEG_{5k}$-PGA_{50} (**2**) were mixed in 1 mL acetone/H_2O (*v/v* 1:1) solution to self-assemble into OPNPs via formation of the COO-Pt coordination bonds.[46-49] In this solution, the molar ratio between the Pt contents in **1** and carboxylic groups of **2** is 1:1.7. After 30-min stirring at r.t., the volatile compounds were removed under reduced pressure, and the product was washed with acetone to remove unreacted starting materials. Then, the OPNPs were re-suspended in 1 mL phosphate buffer saline (PBS). The aqueous solution was filtered through a 0.2 µm PTFE syringe filter. The Pt content in the OPNPs was determined by graphite furnace atomic absorption spectroscopy (GFAAS). Notably, a high concentration of Pt (3.2 mM) was obtained in the PBS solution of OPNPs. In contrast, the organoplatinum building block (**1**) has a very low solubility in PBS (88.0 µM at r.t.). The yield of the nanoformulation was determined as 80.8%. The purified nanoparticles were further characterized by TEM and dynamic light scattering (DLS). In the TEM image (Fig 2A and Fig S1 in the supporting information), the core of the nanoparticles formed via aggregation of organoplatinum building blocks was observed. They were mostly spherical in shape, and their size ranged from 95 to 160 nm with an average size of 128 nm. According to the DLS data (Fig 2B and Fig S2), the overall size of the nanoparticles including the peripheral polymers is approximately 134 nm. The zeta-potential was determined to be -2.33 mV (Fig 2C). To assure stability in aqueous solution, the newly prepared nanoparticles were placed in an aqueous solution and size measurements were recorded over 5 days. The DLS data (Fig 2B) indicates that no significant changes in size had occurred. In summary, we have successfully prepared organoplatinum polymeric nanoparticles (OPNPs)that are stable in aqueous solution and enhance the solubility and biocompatibility of the hydrophobic organoplatinum complex.

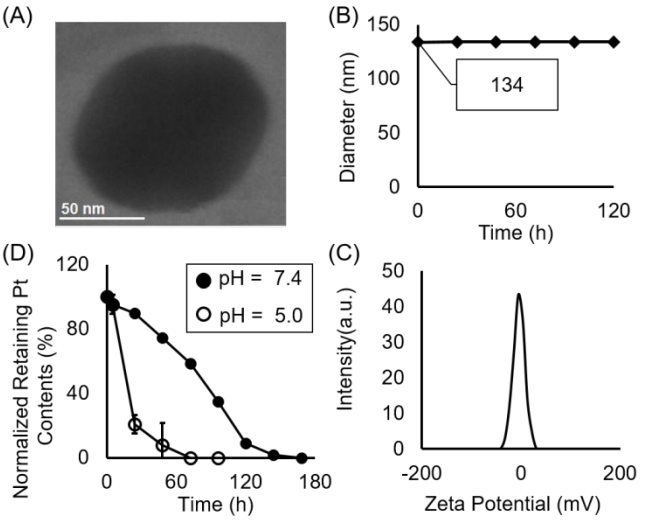

Figure 2. Characterization of OPNPs: (A). a representative TEM image of OPNPs; (B). DLS of OPNPs in PBS over 5 days at r.t.; (C). zeta-potential of OPNPs in PBS; (D). Pt payload release profiles of OPNPs in PBS (pH = 7.4) and acetate buffer (pH = 5.0).

Cytotoxicity profiles. The *in vitro* anticancer activity of OPNPs was assessed using the 3-(4,5-dimethylthiazol-2-yl)-2,5-diphenyltetrazolium bromide (MTT) assay. A panel of human cancer cell lines were employed in this study, including A549 (lung cancer), A2780, A2780cis and SKOV3 (ovarian cancer), MDA-MB-231 (breast cancer). The cells were treated with cisplatin, **1**, or OPNP for 72 h and cell viability was evaluated. In our previous study, we had confirmed that **2** is non-toxic against the cell lines used in this study. The IC_{50} values, which represent the concentration of the drug required to inhibit growth of cells by 50%, are reported in the table (Fig 3A). The results show that OPNPs have lower IC_{50} values compared to those of cisplatin. For example, in the A549 lung cancer cell line, the IC_{50} (OPNPs) = 2.57±0.30µM is 3 times lower than that of cisplatin (IC_{50} = 7.40±2.71µM). A2780 (cisplatin-sensitive) and A2780cis (cisplatin-resistant) are a pair of ovarian cancer cell lines that are commonly used to evaluate the resistance factor (RF) using $IC_{50(A2780cis)}/IC_{50(A2780)}$. As a result (Fig 3A and 3B), the value of the RF for cisplatin is 23.8, and the value of RF(OPNPs) is 0.78, indicating no cross-resistance between cisplatin and the OPNPs. The *in vitro* anticancer activity of OPNPs was further studied by LIVE/DEAD cell assay using fluorescent microscopy (a combination of the ethidium homodimer (Erb) and a staining of acetomethoxycalcein, or calcein AM). Live cells were stained with calcein AM and yield a green fluorescence signal, whereas dead cells exhibit no fluorescence or a red signal due to the ethidium homodimer. A2780cis cells treated with OPNP ([Pt] = 6 µM) for 24 h exhibit significant cell death, but those treated with cisplatin under the same conditions are all survived (Fig 3C). Overall, we conclude that the OPNPs are more potent than cisplatin, and they are capable of overcoming drug resistance in ovarian cancer.

(A)

IC_{50} (μM)	A2780 Ovarian Cancer Sensitive to cisplatin	A2780cis Ovarian Cancer Resistant to cisplatin	SKOV-3 Ovarian Cancer	A549 Lung Cancer	RF $\frac{IC_{50(A2780cis)}}{IC_{50(A2780)}}$
Cisplatin	1.22 ± 0.27	29.0 ± 4.01	34.26 ± 5.03	7.40 ± 2.71	23.8
1	0.31 ± 0.12	1.59 ± 0.62	8.74 ± 2.57	4.67 ± 1.85	5.13
OPNP	4.09 ± 0.89	3.19 ± 0.44	11.72 ± 4.87	2.57 ± 0.30	0.780

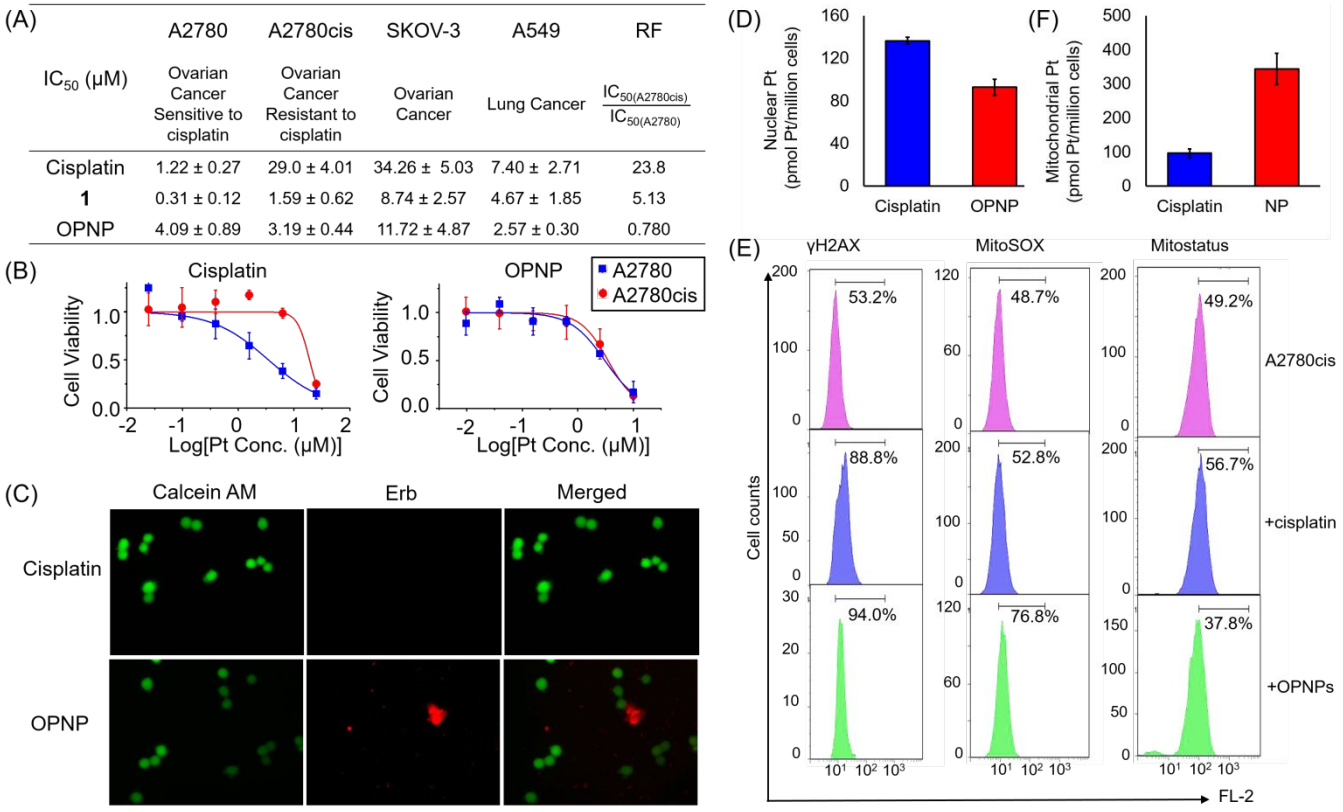

Figure 3. Cellular responses of OPNPs: (A) Cytotoxicity profiles of cisplatin, organoplatinum complex 1, and OPNPs against a panel of human cancer cell lines (72 h, RF=resistance factor); (B). representative killing curves of cisplatin and OPNPs against A2780 (cisplatin-sensitive) and A2780cis (cisplatin-resistant) ovarian cancer cell lines; (C). images of LIVE/DEAD cell assays of A2780cis cells treated with cisplatin or OPNPs ([Pt] = 6 μM, 24 h); (D). nuclear Pt contents in A2780cis cells treated with cisplatin or OPNPs; (E). flow cytometric analysis of γH2AX (*left*), MitoSOX (*middle*), and Mitostatus (*right*) of A2780cis cells treated with cisplatin or OPNPs; (F). mitochondrial Pt contents in A2780cis cells treated with cisplatin or OPNPs ([Pt] = 20 μM, 3 h).

Cellular uptake. To better understand the origin of the superior therapeutic effects of the OPNPs, we sought to investigate the mechanism of action of these nanoparticles. In general, cell entry represents the first step of the process. We utilized GFAAS to study the cell entry by analysing the intracellular Pt contents. In the experiment, one million A2780cis cells were treated with OPNPs, **1**, and cisplatin ([Pt] = 20 μM). After 3 h, the cellular Pt contents were determined using GFAAS. The results (Fig. S3) show that the cellular uptake of cisplatin was only 50.1 ±1.1 pmol/millon cells, while the uptake of OPNPs were 7 times higher (344.7±13.1 pmol/million cells). The results indicate that the OPNPs facilitate the cell entry of the organoplatinum payloads. Nanoparticles usually enter cells via the process of endocytosis. To confirm that this was occurring with our OPNPs, we carried out the cellular uptake experiments at 4 °C. As expected, the uptake of OPNPs was significantly reduced at 4 °C (79.5±2.7 pmol/million cells) compared to that at 37 °C (344.7±13.1 pmol/million cells). For cisplatin, no significant changes were observed. To sum up, our data suggest that the OPNPs can readily enter cells via endocytosis, therefore shuttling a large payload of organoplatinum complexes into the cancer cells.

Payload release. Next, we studied the drug release of OPNPs. Since endosomes are acidic (pH = 5.0–6.5) subcellular organelles, we are particularly interested in how the OPNPs release the payload under acidic conditions. In the experiment, drug releasing profiles of the OPNPs were studied in PBS (pH = 7.4) and acetate buffer solution (pH = 5) using micro-dialysis bags (3.5 kDa MWCO). In Fig 2D, the OPNPs show a very slow release in PBS (pH = 7.4), and only 25% of the encapsulated payloads were released after 50 h. On the other hand, the OPNPs exhibits much faster release of Pt contents in acidic media. About 80% of the Pt contents were released in the acetate buffer solution after 20 h. These results indicate that the therapeutic contents remain encapsulated within the OPNPs before entering cells and then readily released in the acidic environment of endosomes.

Nuclear accumulation and DNA damage. To further explore the intracellular targets of the organoplatinum compound, we first investigated the potential of OPNPs triggering nuclear DNA damage, which is a common killing mechanism among metallodrugs.[3] First, we examined whether the Pt payloads can reach the nucleus after their release from inside the endosomes. In the experiment, A2780cis cells

were incubated with cisplatin and OPNP ([Pt] = 20 μM) for 3h. The nuclei of the treated cells were isolated by centrifugation with 0.1% NP-40 (nonionic polyoxyethylene surfactant) PBS solution. The Pt contents in these isolated nuclei were measured by GFAAS. As a control, the cisplatin-treated cells have 136.35±3.30 pmol Pt/million cells in their nuclei (Fig 3D). Notably, in the OPNP-treated cells, there are 92.79±7.49 pmol Pt/million cells found in their nuclei, similar to that of cisplatin. We then examined the DNA damage caused by the organoplatinum payloads. γH2AX and phosphorylated H2AX are a biomarkers of nuclear DNA damage. In the experiment, we first treated the A2780cis cells with cisplatin or OPNPs, and then carried out flow cytometric analysis of γH2AX of these cells[26]. As shown in Fig 3E (left), the OPNP-treated cells show a similar level of γH2AX compared to that of cisplatin, which is consistent with the abovementioned results in nucleus uptake. Furthermore, we used NMR spectroscopy and mass spectrometry to probe the interaction between the organoplatinum compound and DNA nucleotides. We hypothesize that **1** is able to interact with guanine via formation of Pt-N bonds (Fig S4 in SI). Compound **1** (8.5 mg, 7.6 μmol) and guanine (6.0 mg, 40. μmol) were mixed in 0.7 mL DMSO-d_6 at r.t.. The insoluble free guanine was removed by filtration. In the ^{31}P NMR spectra (Fig S4), the singlet at 16.12 ppm was upfield shifted comparing to that of Compound **1** (20.91 ppm), indicating the formation of Pt-N bonds.[43,44] In the MS spectrum (Fig S6), the peaks corresponding to the coordination product were also observed. The evidence collectively suggests that the Pt payloads can reach nuclei in cancer cells and trigger DNA damage.

Mitochondrial accumulation and damage. Mitochondria emerge as an important target toward overcoming drug resistance in ovarian cancer.[50, 51] To explain the superior therapeutic effects of the OPNPs, we further analysed their capability of accumulating in and damaging mitochondria. In particular, mitochondrial Pt uptake of A2780Cis cells was tested after incubation with OPNPs or cisplatin ([Pt] = 20 μM) for 3 h. Mitochondria were isolated with a commercially available mitochondria isolation kit, and the Pt contents were measured by GFAAS. In Fig 3F, the results show that the mitochondrial uptake of cisplatin is only 96.0±12.2 pmol/million cells, while that of OPNPs was 343.3±45.9 pmol/million cells. These results verify that the organoplatinum payloads more effectively accumulate in mitochondria than cisplatin does. Next, we carried out flow cytometric analysis of mitochondrial damage based on MitoSOX™ and MitoStatus™ assays. Mitochondrial superoxide was monitored by MitoSOX Red, a mitochondrial superoxide indicator. As shown in Fig 3E (middle), a higher intensity of fluorescence signal was observed in the OPNP-treated cells compared to that of the control. Likewise, flow cytometric analysis of MitoStatus was performed to monitor the change in mitochondrial membrane potential. A healthy mitochondrial membrane is negatively charged, and the potential ($\Delta\Psi_m$) is lowered when damaged by toxins. Tetramethylrhodamine ethyl ester (TMRE) is a positively charged fluorescence active dye that can stain mitochondria. In the Mitostatus assay, TMRE was used as a stain to monitor the change of $\Delta\Psi_m$. As shown in Fig 3E (right), the $\Delta\Psi_m$ was significantly lowered in the OPNP-treated cells compared to that of the untreated cells. In sum, GFAAS and flow cytometric analysis indicate that the organoplatinum payloads can reach mitochondria and then trigger mitochondrial damage.

Apoptosis. Finally, cellular response was determined by using flow-cytometric analysis of apoptosis. At the early stage of apoptosis, phosphotidyl serine, is present in the inner lipid layer, moves to an outer layer. FITC-annexin V is a green fluorescence dye-conjugated antibody that can selectively recognize phosphotidyl serine on the outer membrane, therefore allowing for flow cytometric analysis of apoptosis. By the time of late apoptosis, membranes get damaged and allow molecules to penetrate in. Therefore, during late apoptosis propedium iodide (PI) dye molecules can penetrate into damaged cells and give a red signal in flow cytometry analysis. The occurrence of apoptosis in the OPNP-treated A2780cis cells was studied using a dual staining annexin V/PI flow cytometric assay. The results in Fig 4 clearly indicate that OPNPs have effectively induced apoptosis in A2780cis cisplatin-resistant ovarian cancer cells. After incubating cells with OPNPs ([Pt] = 6 μM) for 72 h, a large population of cells were in late (17.72%) and early (48.32%) apoptosis stages compared to the effect of 20 μM cisplatin, which only induced 22.14% and 23.54% of cells to undergo late and early apoptosis respectively (Fig 4 and Fig S7 in SI).

Mechanism of action. Fig 5 depicts the proposed mechanism of action of the OPNPs based on the aforementioned cell-based studies. The OPNPs readily enter ovarian cancer cells via endocytosis. Within acidic endosomes, the OPNPs slowly release the organoplatinum contents. These platinum payloads can reach both the nucleus and mitochondria, and induce a "dual-action" attack on nuclear DNA and mitochondria. As a result, the OPNPs can effectively trigger apoptosis in cisplatin-resistant ovarian cancer cells.

Conclusions

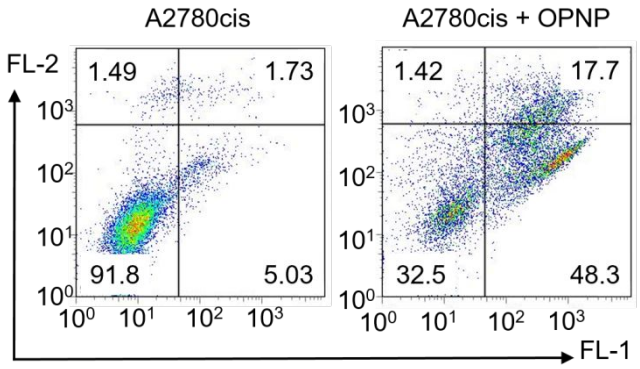

Figure 4. Flow cytometric analysis of apoptotic events in A2780cis cells treated with OPNPs ([Pt] = 6 μM, 72 h).

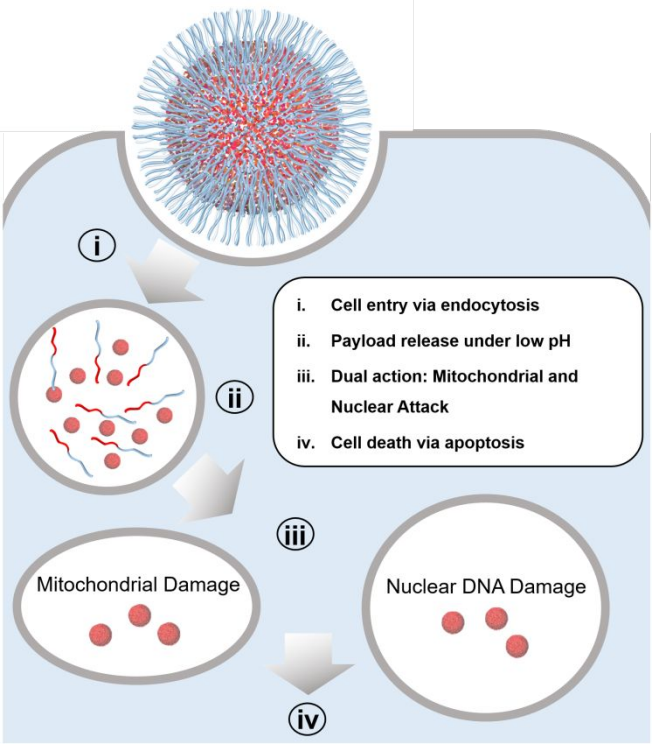

Figure 5. The proposed mechanism of action of OPNPs.

We have presented the development of organoplatinum polymeric nanoparticles to facilitate the "dual-action" attack of cisplatin-resistant ovarian cancer cells. In this study, we demonstrated that the hydrophobic organoplatinum compound (**1**) can be formulated into nanoparticles in the presence of $MPEG_{5k}$-PGA_{50} to enhance its water solubility. The nanoformulation is driven by the coordination interactions between Pt centres and carboxylate groups present in the polymer. Using MTT assays, we found that the OPNPs exhibit promising *in vitro* efficacy against a panel of human cancer cell lines, and notably, the OPNPs show a low resistance factor against a cisplatin-resistant ovarian cancer cell line. Furthermore, we explored the origin of the superior activity of OPNPs. The nanoparticles readily enter cancer cells via endocytosis, and slowly release the therapeutic content (**1**) under acidic conditions. The OPNPs can trigger a "dual-action" attack in both the nucleus and mitochondria. For the research field of bioinorganic chemistry, our research not only provides a first-of-its-kind design of engaging organoplatinum complexes in cancer therapy, but also offers new insights into understanding the mechanism of action of such complexes.

Experimental

General information. All reagents were purchased from Strem, Aldrich or Alfa and used without further purification. $MPEG_{5k}$-PGA_{50} (**2**) was purchased from Polypeptide Therapeutic Solutions SL (Valencia, Spain). The organoplatinum complex (**1**) was synthesized according to the reported literature. All reactions were carried out under normal atmospheric conditions. GFAAS measurements were taken on a PerkinElmer PinAAcle 900Z spectrometer. Fluorescence images were acquired using an Olympus IX70 inverted epifluorescence microscope equipped with a digital CCD camera (QImaging). Images were processed and intensities were quantified with ImageJ software (NIH). Dynamic light scattering and zeta-potential analysis were carried out using a Horiba SZ-100 particle analyzer. Flow cytometry was carried out on a FACSAria™II flow cytometer. TEM specimens were examined using FEI Tecnai F20 TEM.

Formation of organoplatinum polymeric nanoparticles (OPNPs). The organoplatinum complex (**1**) was synthesized using a reported method. A volume of 0.5 mL acetone solution of **1** (2.2 mg, 1.7 µmol) was added to 0.5 mL aqueous solution of $MPEG_{5k}$-PGA_{50} (0.9 mg, 0.12 µmol), and the mixture was stirred for 30 min at r.t. The volatile compounds were removed under reduced pressure. The resulted brown residue was washed twice with 1 mL of acetone under sonication. After removing acetone by centrifugation, the final product of OPNP was dried in vacuum overnight. The OPNPs were re-suspended in 1 mL PBS and filtered via 0.2 µm filter. The final Pt concentration was determined to be 3.2 mM. Yield: 80.8%.

Measurements of drug release profiles. A volume of 1 mL PBS solution (pH = 7.4) or acetate buffer (pH = 5.0) containing OPNP ([Pt] = 100 µM) was sealed in micro-dialysis bags (3.5 kDa MWCO) against 500 mL PBS solution or acetate buffer at r.t. Samples were collected from the dialysis periodically and analyzed with GFAAS. All measurements were done in triplicate.

Cell culture. A2780 and A2780cis cell lines were purchased from Sigma-Aldrich, and cultured in RPMI 1640 with L-glutamine (Corning) supplemented with 10% FBS (Atlanta Biologicals) and 1% Penicillin-Streptomycin (Corning). SKOV-3, MDA-MB-231, A549 cell lines were obtained via American Type Culture Collection, and cultured in DMEM 1 g/L glucose, with L-glutamine & sodium pyruvate (Corning) supplemented with 10% FBS and 1% Penicillin-Streptomycin. All cell lines were cultured at 37°C under an atmosphere containing 5% CO_2. Cells were passaged upon reaching 70–80% confluence by trypsinization and split in a 1:5 ratio.

Cell viability (MTT) assays. Cell viability was determined using 3-(4,5-dimethylthiazol-2-yl)-2,5-diphenyltetrazolium bromide (MTT) assays. Cells were seeded in 96-well microplates in 100 µL cell suspensions ($2x10^4$ cells/mL) per well to begin and were incubated for 24 h at 37°C, 5% CO_2. Next, 50 µL volume of RPMI or DMEM with various concentrations of Pt compounds was added to each well of the microplates. Cells were then incubated an additional 72 h at 37 °C, 5% CO_2. Next, a volume of 30 µL MTT (Alfa Aesar) (5 mg/mL in PBS) was added to the cells and then the cells were incubated an additional 2-4 h at 37°C, 5% CO_2. Solutions were then aspirated, leaving behind insoluble purple formazan. A volume of 200 µL DMSO was

added to wells and plates were shaken for 10 min. Next, the microplates were analyzed for absorbance at 562 nm with an ELx800 absorbance reader (BioTek, Winooski, VT, USA). Finally, the data were analyzed using Origin software to produce dose response curves and to determine IC_{50} values. All experiments were performed in triplicate.

LIVE/DEAD cell viability assays.

The *in vitro* efficacy of cisplatin and OPNP were compared using the LIVE/DEAD cell viability assay (Molecular Probes) in A2780 ovarian cancer cells. A2780cis cells were cultured on 35 mm sterile glass bottom culture dishes (MATTEK corporation) for 24 h at 37 °C and grown in RPMI supplemented with 10% FBS and 1% penicillin/streptomycin. The cells were then treated with 6 μM of Cisplatin or OPNP for 24 h at 37 °C. Before the assay, cells were washed with 1 mL PBS and 1 mL dye-free RPMI to remove serum esterase activity generally present in serum-supplemented growth media. A 5 μL aliquot of calcein AM (4 mM in anhydrous DMSO) and 10 μL ethidium homodimer-1 (2 mM in DMSO/water, 1:4 vol/vol) were added to 10 mL of dye-free RPMI to produce a LIVE/DEAD working solution. A 2 mL aliquot of LIVE/DEAD working solution was carefully added to the petri dishes, which were then incubated at r.t. for 30 min. Subsequently, the medium of the samples was replaced with 1 mL dye-free RPMI before examination by fluorescence microscopy.

Cellular uptake

A2780cis cells were seeded in a 6-well plate at a concentration of 2 x 10^5 cells/well and incubated at 37°C overnight. These cells were treated with cisplatin ([Pt] = 20 μM) and OPNP ([Pt] = 20 μM) for 3 h at 37°C or 4°C. The remaining alive cells were harvested by trypsinization and counted. Cells were then digested in 200 μL 65% HNO_3 at r.t. overnight. The platinum content in the cells were analyzed by GFAAS. All experiments were performed in triplicate.

Mitochondrial accumulation.

A2780cis cells were seeded in a 6-well plate at a concentration of 2 x 10^5 cells/well. These cells were then incubated 24hr at 37°C under an atmosphere containing 5% CO_2. Next, cisplatin (20 μM) and OPNP (20 μM) were added to the wells and incubated a further 3h. After the incubation, cells were collected by trypsinization, counted, and the mitochondria were isolated using the Mitochondria Isolation Kit for Mammalian Cells (Thermo Scientific, Rochester, NY, USA). Once isolated, mitochondria samples were digested in 65% nitric acid overnight. The platinum content was analyzed by GFAAS. All experiments were performed in triplicate.

Nuclear accumulation.

A2780Cis cells were seeded in a 6-well plate at a concentration of 2 x 10^5 cells/well and incubated at 37°C overnight. The cells were treated with cisplatin ([Pt] = 20 μM) and OPNP ([Pt] = 20 μM for 3 h at 37°C. The remaining alive cells were harvested by trypsinization and counted. Next, the cells were suspended in 1mL solution of PBS with 0.1% NP-40 followed by centrifugation to dissociate the cell membrane. This step was duplicated. The isolated nuclei were digested in 200 μL 65% HNO_3 at r.t. overnight. The platinum content was analyzed by GFAAS. All experiments were performed in triplicate.

Mitostatus™ (mitochondrial membrane potential) analysis

A2780cis cells were seeded at a cell density of 2x10^5 cells/mL in 6-well plate. After incubating at 37 °C overnight, cells were treated with cisplatin ([Pt] = 20 μM) and OPNP ([Pt] = 20 μM) at 37°C for 24 h. Next, the medium was removed, washed 2 times with 1 mL PBS, and 5 mL fresh medium was added to each well. Then, the cells were stained with 200 nM MitoStatus reagent (BD Biosciences) in the dark at 37 °C for 30 min. The stain-containing medium was aspirated, and remaining live cells were collected by trypsinization. The cells were then re-suspended in PBS containing 0.5% BSA and analyzed using the PE channel on a FACSAria™II flow cytometer (BD Biosciences, Franklin Lakes, NJ, USA).

MitoSOX™ (mitochondrial ROS production) analysis. A2780Cis cells were seeded in a 6-well plate at a concentration of 2 x 10^5 cells/well. These cells were then incubated 24 h at 37°C under an atmosphere containing 5% CO_2. Next, cisplatin ([Pt] = 20 μM) and OPNP ([Pt] = 20 μM) were added to cells and incubated for further 24 h. MitoSOX Red Mitochondrial Superoxide Indicator (Thermo Scientific, Rochester, NY, USA) was then added to cells to reach a concentration of 5 μM and incubated at 37°C for 1h. Cells were then collected, washed with PBS, and resuspended in PBS containing 0.5% BSA. Cell solutions were analyzed using the PE channel on a FACSAria™II flow cytometer (BD Biosciences, Franklin Lakes, NJ, USA).

Flow cytometric analysis of γH2AX. A2780cis cells were cultured on a 6-well plate at a concentration of 2 x 10^5 cells/well for 24 h at 37 °C. The cells were then treated with cisplatin ([Pt] = 20 μM) and OPNP ([Pt] = 20 μM) for 24 h at 37 °C. Next, live cells were collected and 250ul BD Permeabiliaztion solution was added to re-suspend the cells and incubated for 20 min at 4°C. The cell pellet was collected and washed twice with 1mL wash buffer. To the pellet with 50μL of buffer, Alexa 488-anti γH2AX antibody solution was added and incubated in the dark for 60 min at r.t. The final cell pellet was suspended in 200 μL of PBS with 0.5% BSA and analyzed by flow cytometric PE channel on a FACSAria™II flow cytometer (BD Biosciences, Franklin Lakes, NJ, USA).

Apoptosis assays. A2780cis cells seeded in a 6-well plate at a concentration of 2 x 10^5 cells/well and incubated for 24 h at 37°C. Next, the cells were treated with OPNP (2 or 6 μM) and cisplatin (20 μM), while the fourth well was kept as a control. Cells were then incubated for 72h at 37 °C. The medium was collected in clean 15 mL falcon tubes along with washed PBS solution. 1mL trypsin was added to the wells. After 5min, cell

suspensions were transferred to the falcon tubes that contained the media and PBS, and centrifuged at 400–500 g at 4°C for 5min. The cell pellet was re-suspended in 1 mL PBS and the cells were counted. The cell pellet was collected again and the appropriate amount of 1x binding buffer was added to reach a concentration of 10^6 cells/mL. 100 µL cell suspensions were added to new 2 mL eppendorf tubes and 5 µL Annexin V-FITC was added to one tube and 5 µL PI solution was added to other. Cells were gently vortexed and incubated at r.t. for 15min in the dark. 400uL 1x binding buffer was added to each eppendorf tube and the cell suspensions were transferred to flow cytometry tubes. Flow cytometry analysis was done using FL-1 and FL-2 channels on a FACSAria™II flow cytometer (BD Biosciences, Franklin Lakes, NJ, USA).

Conflicts of interest

There are no conflicts to declare.

Acknowledgements

Y.-R. Z thanks the financial support provided by the startup fund, Farris Family Innovation Fellowship, LaunchPad Award provided by Kent State University. M.M. and Y.R. Z wish to acknowledge the National Science Foundation REU program (CHE-1659571) for support.

Notes and references

1. D. Holmes, *Nature*, 2015, **527**, S217.
2. L. Kelland, *Nat. Rev. Cancer*, 2007, **7**, 573-584.
3. D. Wang and S. J. Lippard, *Nat. Rev. Drug Discovery*, 2005, **4**, 307-320.
4. P. A. Vasey, *Br J Cancer*, 2003, **89 Suppl 3**, S23-28.
5. M. Crespo, *J. Organomet. Chem.*, 2019, **879**, 15-26.
6. M. V. Babak and W. H. Ang, *Met. Ions Life Sci.*, 2018, **18**, 171-198.
7. A. Collado, M. Gomez-Gallego and M. A. Sierra, *Eur. J. Org. Chem.*, 2018, **2018**, 1617-1623.
8. S. Jurgens, F. E. Kuhn and A. Casini, *Curr. Med. Chem.*, 2018, **25**, 437-461.
9. C. C. Konkankit, S. C. Marker, K. M. Knopf and J. J. Wilson, *Dalton Trans.*, 2018, **47**, 9934-9974.
10. M. Martinez-Calvo and J. Mascarenas, *Coord. Chem. Rev.*, 2018, **359**, 57-79.
11. S. Thota, D. A. Rodrigues, D. C. Crans and E. J. Barreiro, *J. Med. Chem.*, 2018, **61**, 5805-5821.
12. C. Gaiddon and M. Pfeffer, *Eur. J. Inorg. Chem.*, 2017, **2017**, 1639-1654.
13. O. Karaca, S. M. Meier-Menches, A. Casini and F. E. Kuehn, *Chem. Commun.*, 2017, **53**, 8249-8260.
14. J. Kljun and I. Turel, *Eur. J. Inorg. Chem.*, 2017, **2017**, 1655-1666.
15. S. Samanta, J. Quigley, B. Vinciguerra, V. Briken and L. Isaacs, *J. Am. Chem. Soc.*, 2017, **139**, 9066-9074.
16. C. Hemmert and H. Gornitzka, *Dalton Trans.*, 2016, **45**, 440-447.
17. M. L. Saha, X. Yan and P. J. Stang, *Acc. Chem. Res.*, 2016, **49**, 2527-2539.
18. G. Jaouen, A. Vessieres and S. Top, *Chem. Soc. Rev.*, 2015, **44**, 8802-8817.
19. L. Xu, Y. Wang, L. Chen and H. Yang, *Chem. Soc. Rev.*, 2015, **44**, 2148-2167.
20. B. Bertrand and A. Casini, *Dalton Trans.*, 2014, **43**, 4209-4219.
21. A. Leonidova and G. Gasser, *ACS Chem. Biol.*, 2014, **9**, 2180-2193.
22. N. Cutillas, G. S. Yellol, C. de Haro, C. Vicente, V. Rodriguez and J. Ruiz, *Coord. Chem. Rev.*, 2013, **257**, 2784-2797.
23. G. Gasser and N. Metzler-Nolte, *Curr. Opin. Chem. Biol.*, 2012, **16**, 84-91.
24. F. Schmitt, J. Freudenreich, N. P. E. Barry, L. Juillerat-Jeanneret, G. Suss-Fink and B. Therrien, *J. Am. Chem. Soc.*, 2012, **134**, 754-757.
25. B. Therrien, *Top. Curr. Chem.*, 2012, **319**, 35-56.
26. P. Wang, C.-H. Leung, D.-L. Ma, W. Lu and C.-M. Che, *Chem. - Asian J.*, 2010, **5**, 2271-2280.
27. A. A. Ali, H. Nimir, C. Aktas, V. Huch, U. Rauch, K.-H. Schafer and M. Veith, *Organometallics*, 2012, **31**, 2256-2262.
28. T. Zou, C.-N. Lok, Y. M. E. Fung and C.-M. Che, *Chem. Commun.*, 2013, **49**, 5423-5425.
29. A. Zamora, S. A. Perez, V. Rodriguez, C. Janiak, G. S. Yellol and J. Ruiz, *J. Med. Chem.*, 2015, **58**, 1320-1336.
30. T. Sun, W. Cui, M. Yan, G. Qin, W. Guo, H. Gu, S. Liu and Q. Wu, *Adv. Mater.* , 2016, **28**, 7397-7404.
31. A. Zamora, S. A. Perez, M. Rothemund, V. Rodriguez, R. Schobert, C. Janiak and J. Ruiz, *Chem.- Eur. J.*, 2017, **23**, 5614-5625.
32. G. Yu, M. Zhang, M. Saha, Z. Mao, J. Chen, Y. Yao, Z. Zhou, Y. Liu, C. Gao, F. Huang, X. Chen and P. Stang, *Journal of the American Chemical Society*, 2017, **139**, 15940-15949.
33. S. Datta, S. K. Misra, M. L. Saha, N. Lahiri, J. Louie, D. Pan and P. J. Stang, *Proc. Natl. Acad. Sci. U. S. A.*, 2018, **115**, 8087-8092.
34. G. Yu, S. Yu, M. L. Saha, J. Zhou, T. R. Cook, B. C. Yung, J. Chen, Z. Mao, F. Zhang, Z. Zhou, Y. Liu, L. Shao, S. Wang, C. Gao, F. Huang, P. J. Stang and X. Chen, *Nat. Commun.*, 2018, **9**, 1-18.
35. Y. Yao, R. Zhao, Y. Shi, Y. Cai, J. Chen, S. Sun, W. Zhang and R. Tang, *Chem. Commun.*, 2018, **54**, 8068-8071.
36. K. Singh, A. Gangrade, A. Jana, B. B. Mandal and N. Das, *ACS Omega*, 2019, **4**, 835-841.
37. X. Yan, S. Li, J. B. Pollock, T. R. Cook, J. Chen, Y. Zhang, X. Ji, Y. Yu, F. Huang and P. J. Stang, *Proc. Natl. Acad. Sci. U. S. A.*, 2013, **110**, 15585-15590.
38. F. Zhou, S. Li, T. R. Cook, Z. He and P. J. Stang, *Organometallics*, 2014, **33**, 7019-7022.
39. X. Yan, T. R. Cook, J. B. Pollock, P. Wei, Y. Zhang, Y. Yu, F. Huang and P. J. Stang, *J. Am. Chem. Soc.*, 2014, **136**, 4460-4463.
40. L. Chen, Y. Ren, N. Wu, B. Sun, J. Ma, L. Zhang, H. Tan, M. Liu, X. Li and H. Yang, *J. Am. Chem. Soc.*, 2015, **137**, 11725-11735.
41. Z. Yue, H. Wang, Y. Li, Y. Qin, L. Xu, D. J. Bowers, M. Gangoda, X. Li, H. B. Yang and Y. R. Zheng, *Chem. Commun.*, 2018, **54**, 731-734.
42. J.-H. Tang, Y. Sun, Z.-L. Gong, Z.-Y. Li, Z. Zhou, H. Wang, X. Li, M. L. Saha, Y.-W. Zhong and P. J. Stang, *J. Am. Chem. Soc.*, 2018, **140**, 7723-7729.

43. H.-B. Yang, K. Ghosh, B. H. Northrop, Y.-R. Zheng, M. M. Lyndon, D. C. Muddiman and P. J. Stang, *J. Am. Chem. Soc.*, 2007, **129**, 14187-14189.
44. K. Ghosh, H.-B. Yang, B. H. Northrop, M. M. Lyndon, Y.-R. Zheng, D. C. Muddiman and P. J. Stang, *J. Am. Chem. Soc.*, 2008, **130**, 5320-5334.
45. Y. Wang, M. Zhong, J. Park, A. Zhukhovitskiy, W. Shi and J. Johnson, *J. Am. Chem. Soc.*, 2016, **138**, 10708-10715.
46. K. Singh, S. Kumari, A. Jana, S. Bhowmick, P. Das and N. Das, *Polyhedron*, 2019, **157**, 267-275.
47. G.-Z. Zhao, Q.-J. Li, L.-J. Chen, H. Tan, C.-H. Wang, D.-X. Wang and H.-B. Yang, *Organometallics*, 2011, **30**, 5141-5146.
48. Q.-J. Li, G.-Z. Zhao, L.-J. Chen, H. Tan, C.-H. Wang, D.-X. Wang, D. A. Lehman, D. C. Muddiman and H.-B. Yang, *Organometallics*, 2012, **31**, 7241-7247.
49. A. Jana, S. Mandal, K. Singh, P. Das and N. Das, *Inorg. Chem.*, 2019, **58**, 2042-2053.
50. S. Wisnovsky, J. Wilson, R. Radford, M. Pereira, M. Chan, R. Laposa, S. Lippard and S. Kelley, *Chemistry & Biology*, 2013, **20**, 1323-1328.
51. S. Marrache, R. Pathak and S. Dhar, *Proc. Natl. Acad. Sci. U. S. A.*, 2014, **111**, 10444-10449.

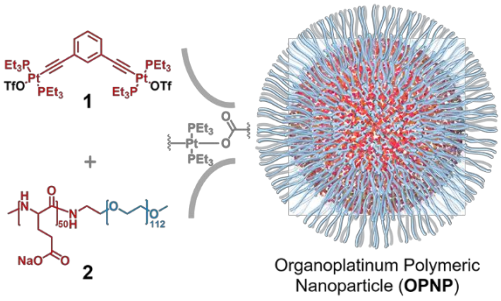

This work demonstrates the development of “dual-action” organometallic polymeric nanoparticles (OPNPs) for treating drug-resistant ovarian cancer.